Available online at www.sciencedirect.com
ScienceDirect
Catalysis Today 136 (2008) 18–27
CATALYSIS TODAY
www.elsevier.com/locate/cattod

Study of a Fe–zeolite-based system as NH_3-SCR catalyst for diesel exhaust aftertreatment

Antonio Grossale, Isabella Nova, Enrico Tronconi *

Dipartimento di Chimica, Materiali e Ingegneria Chimica "G.Natta", Politecnico di Milano, Piazza Leonardo da Vinci 32, 20133 Milano, Italy

Available online 21 December 2007

Abstract

The reactivity of a commercial Fe-exchanged zeolite catalyst is herein analyzed in the NH_3-SCR (selective catalytic reduction) reactions of interest for industrial applications to the aftertreatment of diesel exhausts.

Transient tests, addressing reacting systems of growing complexity ($NH_3 + O_2$, $NO + O_2$, $NO_2 + O_2$, $NH_3 + NO + O_2$, $NH_3 + NO_2 + O_2$ and $NH_3 + NO + NO_2 + O_2$) in a representative temperature range, were performed over the catalyst both in the powder form, in order to derive intrinsic kinetic information, and in the form of small core washcoated monoliths. Results were compared to those collected over a commercial extruded V_2O_5–WO_3/TiO_2 catalyst.

The zeolite system was characterized by: (i) a higher NH_3 storage capacity, (ii) a higher activity in NH_3 and NO oxidation reactions, (iii) a higher activity in the standard SCR reaction at low temperature, (iv) a higher activity in the fast SCR reaction and (v) a higher selectivity to N_2O in the presence of excess NO_2.

© 2007 Elsevier B.V. All rights reserved.

Keywords: Aftertreatment; Diesel–urea SCR; $DeNO_x$; Fast SCR; Fe–zeolite catalysts; V_2O_5–WO_3/TiO_2 catalysts

1. Introduction

Diesel and lean-burn engines are attractive alternatives to stoichiometric Otto engines due to lower fuel consumption and lower CO_2 emissions. Considering the present and moreover the forthcoming regulations for polluting emissions from vehicles, however, one of the main problems that limits diesel engines application is the reduction of NO_x ($NO + NO_2$) which are formed during fuel combustion.

The urea/NH_3 selective catalytic reduction (SCR) technology is considered an effective and proven aftertreatment method to abate NO_x species under lean conditions, i.e. in the presence of excess oxygen. During the last few years several automotive companies, such as DaimlerChrysler, Iveco, Volvo and Renault [1–3], have started to commercialize this technology for the abatement of NO_x emissions from heavy-duty diesel vehicles. The selective catalytic reduction process is based on the reactions between nitrogen oxides and NH_3/urea according to the following main stoichiometries:

$$2NH_3 + 2NO + 1/2O_2 \rightarrow 2N_2 + 3H_2O \quad (1)$$

$$2NH_3 + NO + NO_2 \rightarrow 2N_2 + 3H_2O \quad (2)$$

(1) and (2) are commonly referred to as the standard and the fast SCR reaction, respectively [4–6]. The importance of the fast SCR reaction (2) has recently increased significantly, since the possibility to install an oxidation precatalyst upstream of the SCR converter, thus incrementing the NO_2/NO_x feed ratio, provides an effective chance to boost the low temperature $DeNO_x$ activity of SCR converters for automotive exhaust aftertreatment [7].

The first generation of commercial SCR catalysts for mobile applications were extruded honeycomb monoliths made of a TiO_2 anatase carrier supporting the active components (i.e. typically V_2O_5 and WO_3), similar to the vanadium-based catalysts used for stationary SCR applications [6]. However, the more and more stringent legislation about NO_x emissions, the issues related to vanadium toxicity and the necessity of catalysts active up to higher temperatures have more recently driven the research focus towards new types of catalysts, such

* Corresponding author. Tel.: +39 02 2399 3264; fax: +39 02 2399 3318.
E-mail address: enrico.tronconi@polimi.it (E. Tronconi).

0920-5861/$ – see front matter © 2007 Elsevier B.V. All rights reserved.
doi:10.1016/j.cattod.2007.10.117

as hydrogen- and metal-exchanged zeolites, which had been already proposed in the past for NO_x abatement from stationary installations as well [6–27].

In this work the activity of a commercial iron-exchanged zeolite catalyst for vehicle applications is investigated in the different reactions typical of the SCR reacting system (i.e. in the presence of ammonia, NO, NO_2 and O_2), and the results are compared with those of a previous similar study performed over a commercial V_2O_5–WO_3/TiO_2 catalyst [28–34]. We present results collected over the two catalysts both in the form of powder, obtained by crushing the original honeycomb monoliths, and in the form of core washcoated monolith samples, as well. Crushed monolith tests allow obtaining information about the prevailing network of reactions and their intrinsic kinetics, whereas core monolith runs are analyzed to validate the crushed powder results as an intermediate step to the real full scale. Differences between crushed powder and core monolith results may provide useful indications concerning the role of transport resistances in the monolithic catalyst.

This study is a part of a project aimed at the development of an unsteady, chemically consistent mathematical model of real-scale urea SCR catalytic converters, to be used for design, application and optimization of integrated exhaust after-treatment systems for diesel vehicles [8–10].

2. Experimental

Reactive experiments were performed over a commercial Fe-promoted zeolite SCR catalyst supplied by DaimlerChrysler in the form of a 400 cpsi washcoated honeycomb monolith. The mass fraction of zeolitic active phase was estimated (from the washcoat mass fraction and the measured monolith density) to be 0.262. Different catalyst structures were studied: powdered catalysts, obtained by crushing and sieving (140–200 mesh) the original monolith samples, and small core monolith samples. For comparison purposes, we report also data over a commercial extruded V_2O_5–WO_3/TiO_2 catalyst, again both in the powder and in the monolith form [28,30].

Kinetic experiments were carried out according to transient response methods (TRM) in a tubular microreactor loaded with powdered catalyst: 160 mg of catalyst were typically used. The microreactor consisted of a quartz tube (6 mm i.d.) directly connected in parallel to a quadrupole mass spectrometer (Balzers QMS 200) and to a UV-analyzer (ABB LIMAS 11HV) through lines heated to 200 °C to prevent deposition of ammonium nitrate. The reactor was placed into an electric furnace and a thermocouple directly immersed in the catalyst bed measured the reaction temperature. NH_3, NO, NO_2, O_2 and He feed streams were dosed by mass flow controllers, while water vapour was added by means of a saturator. Helium was used as inert carrier gas in order to allow evaluation of N_2, which is the main SCR product; accordingly, an overall N-balance could be estimated for each run according to the following equation:

$$\text{N-bal} = \frac{100 \times (NH_{3out} + NO_{out} + NO_{2out} + 2 \times (N_{2out} + N_2O_{out}))}{NH_{3in} + NO_{in} + NO_{2in}}$$

The N-balances always closed within ±5% at steady state, with the exception of those runs where formation of NH_4NO_3 was significant: this point is further discussed in the following paragraphs.

The catalyst was conditioned by heating it in a *T*-ramp at 10 °C/min up to 600 °C in 2% O_2 (v/v) and 10% (v/v) H_2O, and keeping it at 600 °C for 1 h.

Temperature programmed desorption (TPD) and temperature programmed reaction (TPR) experiments were performed between 50 and 550 °C with a heating rate of 2 or 10 °C/min, while the reaction dynamics were investigated by TRM runs (step feed) under isothermal conditions within the 150–450 °C *T*-range. Typical feed contents of NO_x and NH_3 were 1000 ppm, always in the presence of O_2 (2%, v/v) and water (1%, v/v). The system was operated at atmospheric pressure with flow rates of 120 or 280 Ncc/min, corresponding to gas hourly space velocity (GHSV) referred to the active phase between 172,000 and 800,000 Ncc/(h g_{cat}). A detailed description of the experimental equipment and procedures can be found in [27,30,34].

The SCR reactions were also investigated over core drilled monolith samples (with square section 11.5 mm × 11.5 mm, and 50 mm length) under isothermal steady-state conditions within the 150–450 °C *T*-range, using a different rig. The catalyst conditioning procedure was the same as for the powder samples. Typical feed concentrations of NO_x and NH_3 were 500–1000 ppm, O_2 2–10% and water 1–10% (v/v), with balance N_2. Analysis of the outlet gases was performed using a UV-analyzer (ABB LIMAS 11HV) directly connected to the reactor outlet via a heated line.

3. Results and discussion

3.1. NH_3–O_2 reacting system

The ammonia storage capacity was evaluated by TRM experiments in the 50–200 °C *T*-range over both the crushed catalyst and the core monolith samples. At constant temperature under a flow of He + O_2 (2%, v/v) + H_2O (1%, v/v), 1000 ppm of ammonia were added to the microreactor feed in a stepwise manner. The integral difference between the inlet and the outlet ammonia concentration profiles versus time provided the estimates of the ammonia storage capacity, which are plotted per gram of active phase at different temperatures in Fig. 1 (solid symbols).

The zeolite system was able to adsorb significant amounts of ammonia, up to 0.75 mmol/g_{cat} at 50 °C; in line with the exothermicity of the adsorption process, the storage capacity decreased on increasing the adsorption temperature, but values close to 0.4 mmol/g_{cat} were still measured at 200 °C. Similar experiments over the core monolith zeolite (open symbols) provided results in good agreement with those collected over the powdered catalyst.

Fig. 1 also shows the results obtained in the case of the commercial vanadium-based SCR catalyst [30]: it clearly appears that the zeolite catalyst was characterized by a higher NH_3 storage capacity than the vanadium catalyst.

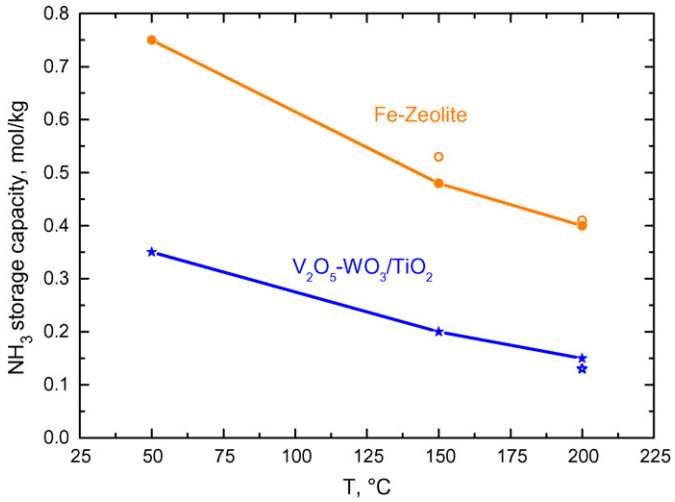

Fig. 1. Ammonia storage capacity of Fe–zeolite and V_2O_5–WO_3/TiO_2 crushed powders (solid symbols) and core monoliths (open symbols).

At the end of the adsorption runs, ammonia was removed from the feed flow, followed by oxygen, and TPD experiments were run by linearly increasing the catalyst temperature at 15 °C/min up to 550 °C in order to completely desorb NH_3 species still adsorbed onto the catalyst surface.

The results of NH_3-TPD runs at 200 °C after catalyst saturation are displayed in Fig. 2 in terms of ammonia outlet concentrations versus temperature for both the zeolite and the vanadium catalyst. Considering the higher load of vanadium-based catalyst as compared to the zeolite (100 mg vs. 42 mg), Fig. 2 confirms the lower adsorption capacity of the vanadium-based system, particularly in the high temperature region. Furthermore, it can be argued that different kinds of ammonia adsorbed species are formed over the two systems, in line with literature indications [11–14] that stronger ammonia adsorbed species could be formed over the zeolite catalyst, which are stable up to higher temperatures.

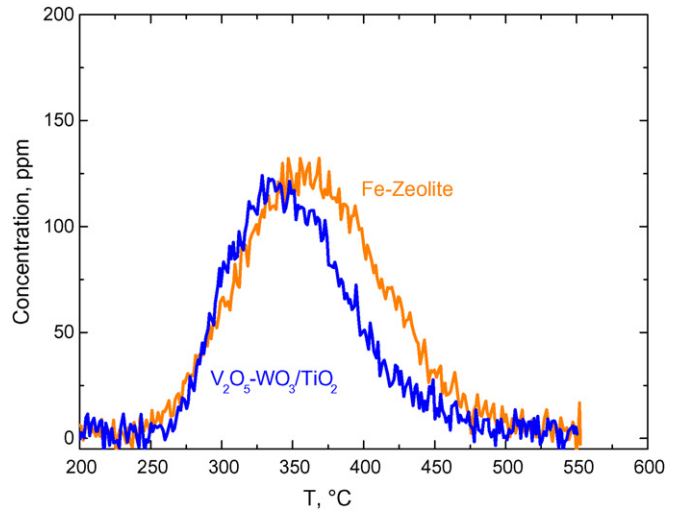

Fig. 2. Ammonia concentration profiles vs. temperature during TPD runs after ammonia adsorption at 200 °C over Fe–zeolite and V_2O_5–WO_3/TiO_2 crushed monoliths. Fe–zeolite crushed monolith: W_{cat} = 0.160 g (0.042 g active phase), Q = 120 Ncc/min. V_2O_5–WO_3/TiO_2: W_{cat} = 0.100 g (0.100 g active phase), Q = 120 Ncc/min. Adsorption: T = 200 °C, NH_3 = 1000 ppm, H_2O = 1%, O_2 = 2%. TPD: T-ramp = 15 °C/min, H_2O = 1%, O_2 = 0%.

The ammonia adsorption capacity was also studied over the zeolite systems in the presence of higher oxygen (2–10%, v/v) and water (1–10%, v/v) concentrations, but no effects were found.

$NH_3 + O_2$ TPR experiments were then performed to study the ammonia oxidation reaction: at room temperature a constant feed of 1000 ppm of ammonia in the presence of 2% (v/v) O_2 and 1% (v/v) H_2O + balance He was admitted to the reactor and then the catalyst temperature was linearly increased with a heating rate of 2 °C/min. The data collected in the case of the zeolite crushed monolith, shown in Fig. 3 in terms of ammonia, nitrogen, NO and NO_2 concentration profiles versus temperature, indicated that ammonia oxidation started around 370–400 °C and proceeded very selectively to nitrogen only according to the following stoichiometry:

$$2NH_3 + 3/2O_2 \rightarrow N_2 + 3H_2O \quad (3)$$

Experimental results were analyzed according to a simplified pseudo first-order rate expression. An apparent activation energy E_{app} of about 20 kcal/mol was estimated in the present case which is lower than in the case of the vanadium-based catalyst ($E_{app} \approx 24$ kcal/mol), in line with a lower activity of the vanadium-based systems in the ammonia oxidation reaction [27].

The effects of water (1–10%, v/v) and oxygen (2–10%, v/v) content on the ammonia oxidation were studied over the zeolite system, as well. Data pointed out an inhibiting effect of water and a promoting action played by oxygen, in line with other literature results collected over metal promoted zeolite systems [14–16].

3.2. $NO–O_2$ and $NO_2–O_2$ reacting systems

The ability of the zeolite system to adsorb and store both NO and NO_2 was then addressed.

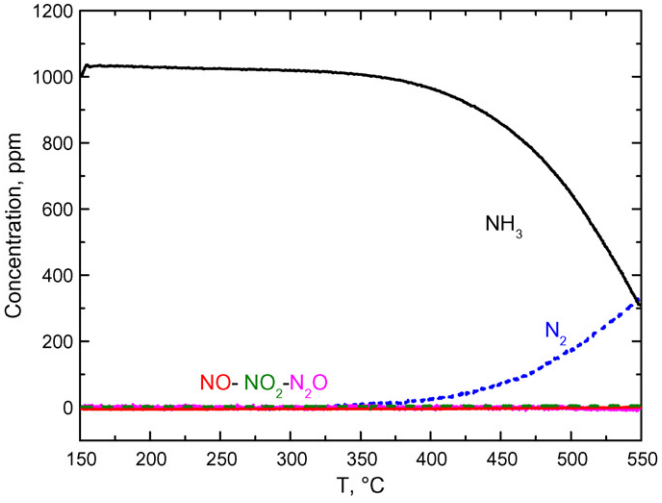

Fig. 3. $NH_3 + O_2$ TPR over Fe–zeolite crushed monolith. W_{cat} = 0.160 g (0.042 g active phase), Q = 120 Ncc/min, NH_3 = 1000 ppm, H_2O = 1%, O_2 = 2%, T-ramp = 2 °C/min.

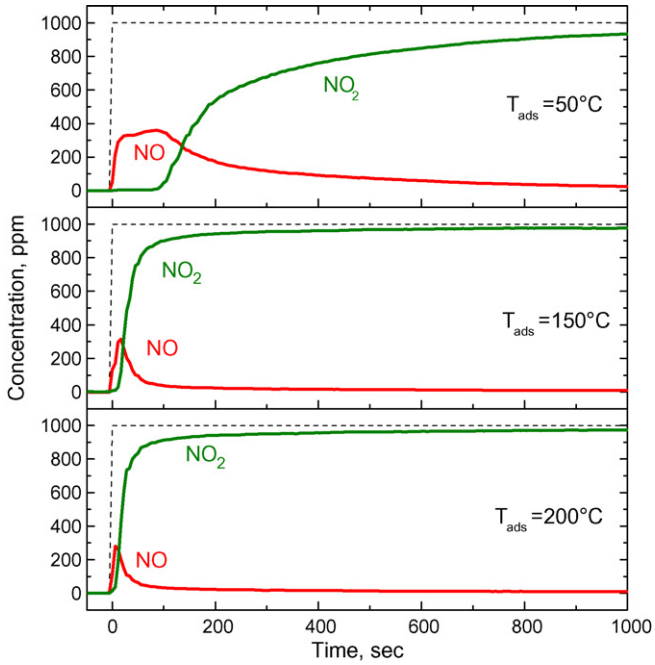

Fig. 4. NO_2 adsorption over Fe–zeolite crushed monolith. W_{cat} = 0.160 g (0.042 g active phase), Q = 120 Ncc/min, NO_2 = 1000 ppm, H_2O = 1%, O_2 = 2%.

The NO adsorption tests were run in the 50–200 °C temperature range, either in the presence or in the absence of oxygen, but no significant adsorption was evident over the zeolite catalyst.

A different picture was observed in the case of NO_2. Fig. 4 shows the results of NO_2-TRM experiments at 50, 150 and 200 °C. In all cases at t = 0 s 1000 ppm of NO_2 were admitted to the microreactor in the presence of O_2 (2%) and H_2O (1%): immediately, NO evolution was observed, while the outlet concentration of NO_2 exhibited a delay before slowly approaching the feed level.

The observed behaviour is in line with the occurrence of NO_2 disproportion according to the global reaction (4), which indeed results from the sum of reactions (4a) and (4b):

$$3NO_2 + O^{2-} \rightarrow 2NO_3^- + NO \quad (4)$$

$$2NO_2 + O^{2-} \rightarrow NO_2^- + NO_3^- \quad (4a)$$

$$NO_2^- + NO_2 \rightarrow NO_3^- + NO \quad (4b)$$

The overall reaction (4) leads to formation of surface nitrates, together with evolution of 1 mol of NO for every 3 mol of adsorbed NO_2. Indeed, inspection of Fig. 4 confirms that the molar ratio between evolved NO and converted NO_2 was always close to 1/3. Fig. 4 also shows that increasing the adsorption temperature resulted in a lower storage capacity: indeed, NO peaks were smaller and correspondingly the NO_2 dead times were shortened.

The capacity to store surface nitrate species via NO_2 disproportion is not peculiar of zeolite systems [17]; indeed it was reported for V_2O_5–WO_3/TiO_2 catalysts, for TiO_2, and for alumina-based systems as well [31,35–38].

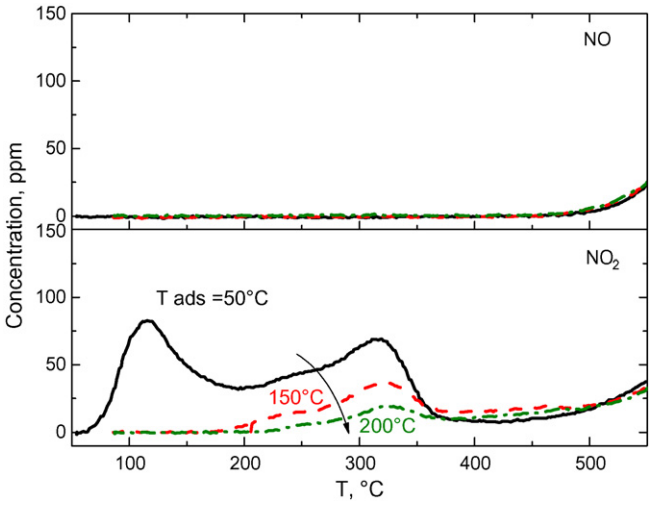

Fig. 5. NO and NO_2 concentration profiles vs. temperature during TPD runs after NO_2 adsorption at 50, 150 and 200 °C over Fe–zeolite crushed monolith. W_{cat} = 0.160 g (0.042 g active phase), Q = 120 Ncc/min. Adsorption: T = 50, 150, 200 °C, NO_2 = 1000 ppm, H_2O = 1%, O_2 = 2%. TPD: T-ramp = 15 °C/min, H_2O = 1%, O_2 = 0%.

At the end of the NO_2 adsorption runs, the thermal stability of the adsorbed nitrates was studied by TPD runs (Fig. 5). Nitrates decomposition led to evolution of NO_2, NO and oxygen (not reported in the figures). When the adsorption was carried out at 50 °C a first desorption peak of NO_2 was observed at low temperatures, probably related to physisorbed species. Then, the main decomposition peak was detected immediately after 300 °C, independently from the adsorption temperature. Above 450 °C, the NO_2 concentration increased again together with that of NO. This behaviour is in line with what expected from decomposition of surface nitrate species [39].

The NO_2 storage capacity was also investigated in the presence of higher contents of water (10%, v/v) and oxygen (10%, v/v): water promoted the capacity of the zeolite system to adsorb nitrate species, while the same was inhibited on increasing the oxygen concentration.

To analyze the activity of the zeolite system in the direct and reverse NO oxidation reaction (5) [15,16,18–21]

$$NO + 1/2O_2 \leftrightarrow NO_2 \quad (5)$$

TPR runs were performed over the crushed monolith, feeding either NO or NO_2 (1000 ppm) in the presence of O_2 (2%) and water (1%) in He. Fig. 6 reports the results of NO oxidation runs in terms of NO and NO_2 outlet concentrations versus temperature. The chemical equilibrium values are also plotted for reference purposes. According to Fig. 6 NO_2 formation started very slowly around 200 °C, reaching a maximum NO conversion of roughly 6% at 500 °C. Above this temperature thermodynamic equilibrium was approached. These data were confirmed by the tests performed over the core zeolite monolith samples. In contrast, the vanadium-based catalyst showed no significant activity in NO oxidation [29,31].

On the other hand, when NO_2 was fed to the reactor in the presence of O_2 (2%) and water (1%) in He, its decomposition to NO started at temperatures higher than 250 °C.

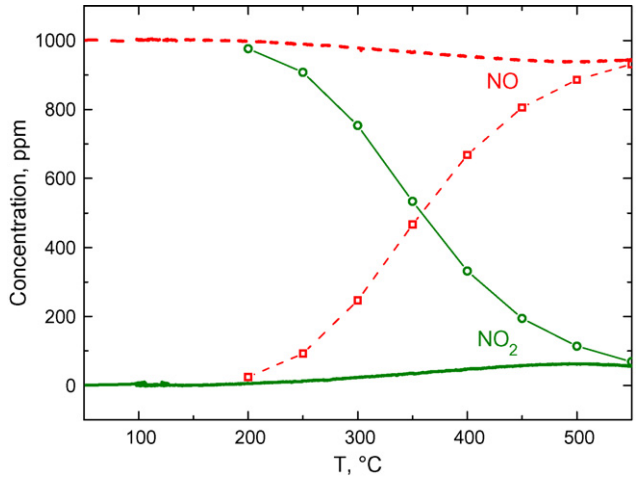

Fig. 6. NO + O_2 TPR over Fe–zeolite crushed monolith. W_{cat} = 0.160 g (0.042 g active phase), Q = 120 Ncc/min, NO = 1000 ppm, H_2O = 1%, O_2 = 2%, T-ramp = 2 °C/min. Solid lines: experimental results, symbols: thermodynamic equilibrium values.

Experiments were also performed to analyze the effects of higher water and oxygen feed contents: as in the case of the ammonia oxidation reaction, it was found that water inhibited the NO oxidation and the NO_2 decomposition as well, while a promoting effect of oxygen was observed for NO oxidation, in line with [12,14].

3.3. NH_3–NO–O_2 reacting system

The reactivity of NO and ammonia in the presence of O_2 (2%, v/v) and H_2O (1%, v/v) was first studied under steady-state conditions: 1000 ppm of NH_3 and 1000 ppm of NO were continuously fed to the reactor and the temperature maintained at desired values until the outlet concentrations of reactants and products reached steady state. Fig. 7 compares the results collected over the zeolite crushed powder (solid lines) and the core monolith samples (dashed lines). In any case, the activity

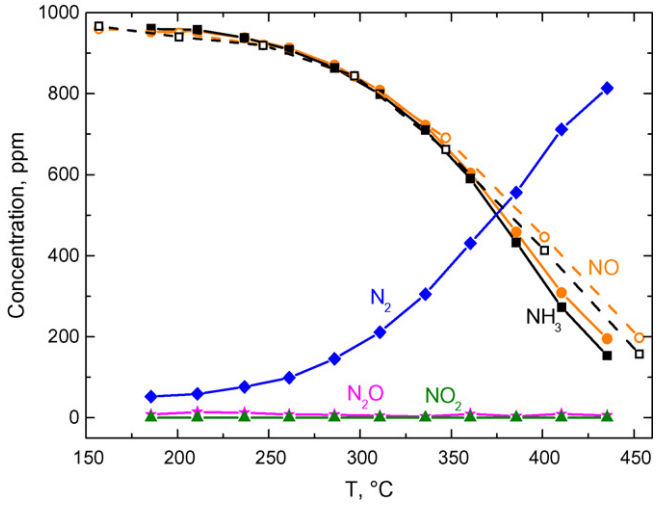

Fig. 7. Standard SCR steady-state results over Fe–zeolite catalyst: crushed powder (solid symbols) vs. core monolith (open symbols). Q = 120 Ncc/min, NH_3 = 1000 ppm, NO = 1000 ppm, H_2O = 1%, O_2 = 2%.

started around 200 °C: NO and ammonia conversions increased with temperature, approaching roughly 80% around 430 °C.

The results over the crushed monolith indicated formation of nitrogen only in the whole investigated T-range. The concentrations profiles of NO, ammonia and nitrogen were in line with the occurrence of the standard SCR reaction (1); however, at temperatures higher than 350 °C a small deviation in the expected 1/1 NO/NH_3 molar consumption ratio was observed, possibly related to the onset of the ammonia oxidation, which was found indeed active in this temperature range (see Fig. 3). The nitrogen production was in fact increased with respect to the expected value of the standard SCR reaction, and in line with the simultaneous occurrence of the two reactions. Similar results have been reported in the literature for several zeolite SCR catalysts [15,16,18,21–24].

The data were analyzed according to pseudo first-order kinetics for NO: from the Arrhenius plots, an E_{app} estimate for the standard SCR reaction close to 13 kcal/mol was derived [18]. A higher apparent activation energy (about 16 kcal/mol) was estimated over the vanadium-based catalyst under similar experimental conditions [32].

Inspection of Fig. 7 also shows that results collected over the monolith sample (dashed lines) were very similar with those of the crushed monolith (solid lines), being almost superimposed up to 350–370 °C; afterwards, the concentrations measured over the monolith were higher, suggesting the onset of diffusional limitations.

Additional experiments were run to analyze the effects of oxygen (2–10%, v/v) and water (1–10%, v/v) feed contents on the standard SCR reaction. It was found that a slight promoting effect of oxygen on the SCR activity was apparent in the whole investigated T-range; it was estimated that the reaction order of oxygen was around 0.4. In contrast, no significant influence of the water feed content was observed.

The standard SCR reaction was finally addressed by dynamic methods performing TRM experiments, i.e. imposing step perturbations in the NH_3 feed concentration (0 → 1000 → 0 ppm) while flowing 1000 ppm of NO, 2% of O_2, 1% of H_2O with balance He, over the crushed monolith between 200 and 350 °C. Fig. 8 shows the results of a dynamic experiment at 250 °C: the measured temporal evolutions of NH_3, NO, N_2 and N_2O outlet concentrations are plotted.

At t = 0 s 1000 ppm of NH_3 were instantaneously added to the reactor feed while flowing 1000 ppm of NO in He: the NO concentration quickly decreased due to reaction with NH_3, passed through a minimum and then approached a steady-state level corresponding to roughly 10% conversion. The N_2 trace followed that of NO as a mirror image, while the NH_3 outlet concentration trace exhibited a dead time before growing up to 900 ppm with very slow dynamics. When the NH_3 feed was shut down (t = 2350 s ca.), the NH_3 trace showed a quick drop, while the NO concentration went through a minimum and then began to increase, eventually reaching the feed value when the reaction was depleted. Again, nitrogen evolution mirrored that of NO.

Similar transient features at ammonia startup and shut down have been also outlined in the SCR literature for different

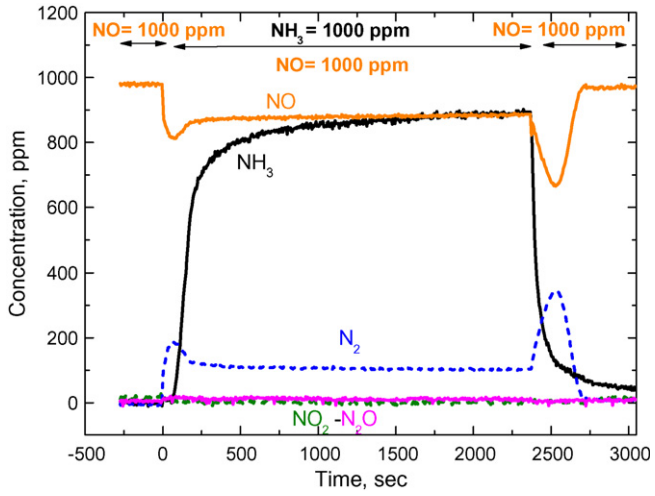

Fig. 8. NO + NH_3 TRM run over Fe–zeolite crushed monolith at 250 °C. W_{cat} = 0.160 g (0.042 g), Q = 120 Ncc/min, NH_3 = 1000 ppm, NO = 1000 ppm, H_2O = 1%, O_2 = 2%.

zeolite systems [24,32], and have already been observed, though less marked, in the case of the vanadium-based catalyst [27,29]. They were explained invoking an inhibiting effect of ammonia. Accordingly, the present transient data in Fig. 8 suggest that the same inhibiting effect occurs, and is actually even more marked, also over zeolite-based SCR catalytic systems.

Such a hypothesis was confirmed by additional TRM experiments run in the presence of excess ammonia (NH_3 = 1200 ppm, NO = 1000 ppm, O_2 = 2%, H_2O = 1% with balance He), which resulted in lower steady-state NO conversions if compared with data collected feeding the stoichiometric 1/1 NO to ammonia feed ratio.

In order to compare the standard SCR activity of the Fe–zeolite to that of the vanadium catalysts, monolith samples were tested under different experimental conditions: in a first set of runs, the same feed flow rates were adopted over two honeycomb samples with equal overall volumes, whereas in a second set of runs the feed flow rates were adjusted to give the same space velocity referred to the catalytically active mass for both systems. It is worth reminding here that the vanadium-based extruded monolith catalyst had 300 cpsi/12.5 mils whereas the zeolite catalyst was coated on a monolith substrate with 400 cpsi/6.5 mils.

The results are depicted in Fig. 9A and B, respectively, in terms of NO and ammonia conversions versus temperature. When comparing the catalysts on the basis of equal volumetric space velocity, which corresponds to using the same overall volume of catalysts, the vanadium-based catalyst was much more active than the zeolite system. Indeed, this is not surprising as the vanadium-based catalyst is an extruded monolith while the zeolite monolith is a washcoated one, thus it includes a lower amount of active phase per unit volume. Conversely, the comparison of the two systems when the same flow rate per gram of catalytically active material was used pointed out that the two systems exhibited similar activities at low temperature, but for $T > 300$ °C the vanadium system

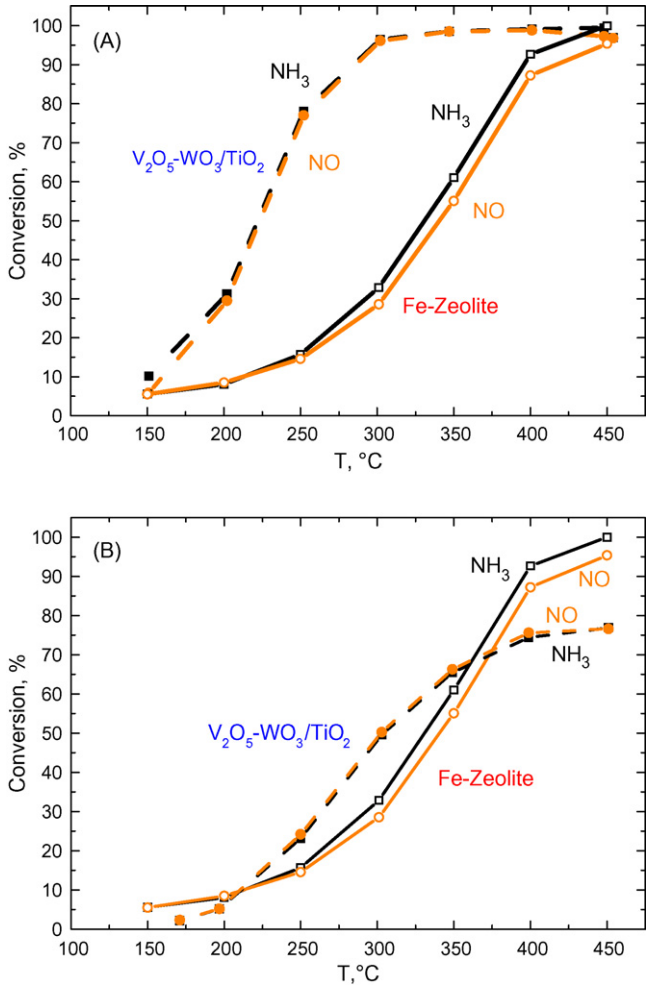

Fig. 9. Standard SCR steady-state results over Fe–zeolite vs. V_2O_5–WO_3/TiO_2 core monoliths. NH_3 = 1000 ppm, NO = 1000 ppm, H_2O = 1%, O_2 = 2%. (A) At constant volumetric GHSV = 27,000 1/h. (B) At constant mass GHSV = 170,000 Ncc/h $g_{active\ phase}$.

resulted in lower conversions, which could be related to the onset of mass transfer limitations possibly due to the lower cell density (300 cpsi vs. 400 cpsi).

3.4. NH_3–NO_2–O_2 reacting system

The crushed monolith zeolite system was then tested in the presence of NO_2 and ammonia. The steady-state results collected in TRM experiments feeding 1000 ppm of NO_2, 1000 ppm of NH_3, 2% (v/v) O_2 and 1% (v/v) H_2O at different temperatures in the range 175–400 °C are summarized in Fig. 10, where the outlet concentrations of NH_3 (filled squares), NO (circles), NO_2 (triangles), N_2O (stars) and the N-balance (open squares) are plotted. Data collected between 175 and 250 °C showed a similar consumption (about 600–650 ppm) of both NH_3 and NO_2 with a production of 350–400 ppm of N_2. N_2O production was negligible up to 200 °C, but almost 200 ppm were detected at 250 °C. Correspondingly, a lack of about 400 ppm in the N-balance was apparent below 200 °C.

At temperatures higher than 250 °C, the situation was dramatically changed: NO_2 and ammonia conversions

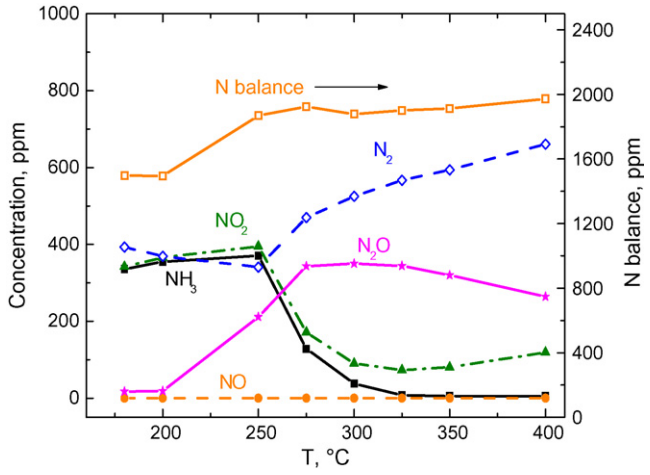

Fig. 10. NO_2 SCR steady-state results over Fe–zeolite crushed monolith. W_{cat} = 0.080 g (0.021 g), Q = 280 Ncc/min, NH_3 = 1000 ppm, NO_2 = 1000 ppm, H_2O = 1%, O_2 = 2%.

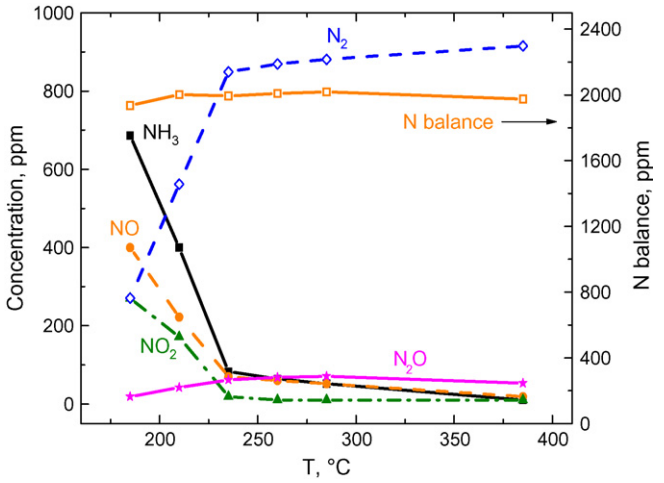

Fig. 11. Fast SCR steady-state results over Fe–zeolite crushed monolith. W_{cat} = 0.160 g (0.042 g), Q = 280 Ncc/min, NH_3 = 1000 ppm, NO_x = 1000 ppm, NO = 500 ppm, NO_2 = 500, H_2O = 1%, O_2 = 2%.

increased, ammonia being converted more than NO_2; nitrogen production increased as well, while N_2O formation was maximum between 275 and 325 °C and then decreased. The N-balance was more or less always closed. Similar results have been reported in the case of different zeolite systems [4,40] and for the vanadium-based catalyst [30], as well.

Data shown in Fig. 10 can be explained considering the occurrence below 250 °C of the reaction between ammonia and NO_2 with formation of ammonium nitrate and nitrogen,

$$2NH_3 + 2NO_2 \rightarrow N_2 + NH_4NO_3 + H_2O \quad (6)$$

and at higher temperatures, of the NO_2 SCR reaction,

$$3NO_2 + 4NH_3 \rightarrow 7/2N_2 + 6H_2O \quad (7)$$

The production of N_2O can be also explained considering that it is the terminal product of the thermal decomposition of ammonium nitrate,

$$NH_4NO_3 \rightarrow N_2O + 2H_2O \quad (8)$$

[4,30,39–41]: accordingly, part of the formed ammonium nitrate decomposes to N_2O.

The results shown in Fig. 10 for the crushed monolith powder were confirmed by data obtained over core monolith samples (not reported).

3.5. NH_3–NO–NO_2–O_2 reacting system

Finally, the activity of the zeolite catalyst was tested in the presence of 1000 ppm of NH_3 and 1000 ppm of NO_x = -NO + NO_2, with different NO/NO_2 feed ratios. In all cases, oxygen (2%, v/v) and water (1%, v/v) were also added to the He carrier gas.

The steady-state results collected over the crushed monolith from TRM runs at different temperatures and for the equimolar 1/1 = NO/NO_2 feed ratio are shown in Fig. 11.

Inspection of the figure points out that at low temperatures the activity of the catalyst was strongly temperature dependent: in fact, at 180 °C a NO_x conversion around 30% was measured, but already at 230 °C conversions close to 90% were obtained. At $T > 250$ °C the activity remained roughly constant. It is also important to notice that NO and NO_2 were not converted in equimolar amounts: the NO_2 outlet concentration was always lower than that of NO, and at $T > 230$ °C NO_2 was almost completely depleted. The main reaction product was nitrogen, even if N_2O was also detected, with a maximum production of 70 ppm between 250 and 300 °C.

The steady-state outlet concentrations of the observed species were in line with the occurrence of the fast SCR reaction (2): this is clearly evident for the high temperature range, where conversions of both NO and NO_2 were complete, and where the evolutions of ammonia and nitrogen were mirror-like, as expected according to stoichiometry (2) [15–19,42].

However, to explain the higher NO_2 conversions observed at low temperature also reaction (6), that is the formation of ammonium nitrate, has to be taken into account. Indeed, in this case outlet concentrations of reactants and products were in line with the simultaneous occurrence of both reactions (2) and (6); moreover N_2O production at higher temperatures was observed, possibly deriving from NH_4NO_3 formation followed by rapid decomposition.

Similar results were obtained also when testing the core monolith zeolite catalyst. In addition, in order to compare the activities of Fe–zeolite and vanadium-based catalysts in the presence of equimolar NO/NO_2 feed mixtures, monolith samples were tested under different experimental conditions, maintaining constant either the volumetric space velocity or the space velocity referred to the catalytic active mass. The results are depicted in Fig. 12A and B, respectively, in terms of NO_x and ammonia steady-state conversions versus temperature. In any case the Fe–zeolite system was associated with a higher activity with respect to the vanadium catalyst, particularly at low temperatures.

The effect of different NO_2/NO_x feed contents (NO_2/NO_x = 0.25, 0.75) was investigated over the crushed monolith

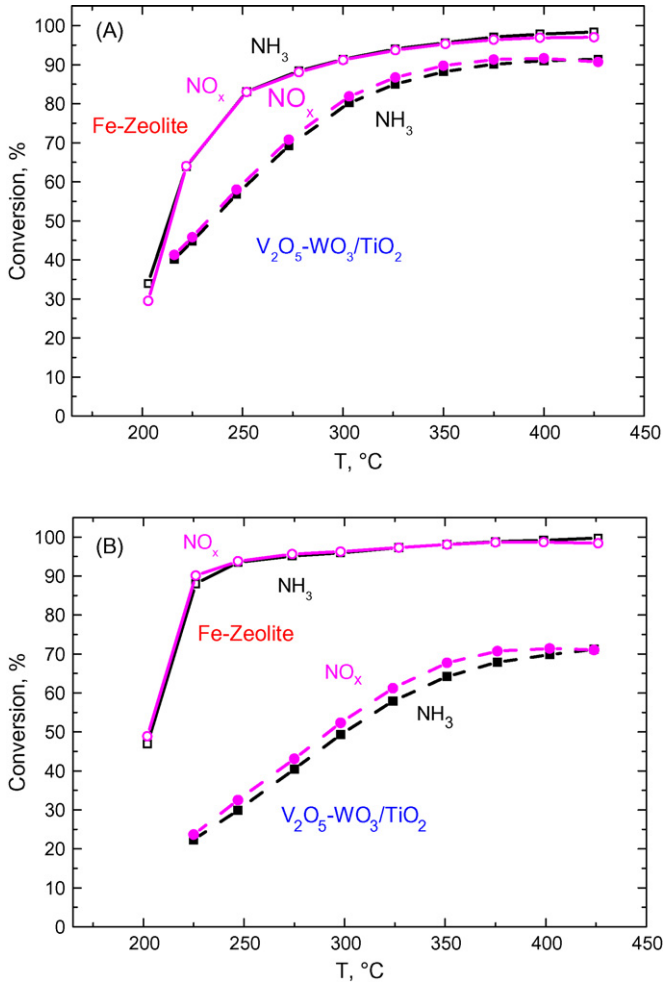

Fig. 12. Fast SCR steady-state results over Fe–zeolite vs. V_2O_5–WO_3/TiO_2 core monoliths. NH_3 = 1000 ppm, NO = 500 ppm, NO_2 = 500 ppm, H_2O = 1%, O_2 = 2%. (A) At constant volumetric GHSV = 126,000 1/h. (B) at constant mass GHSV = 395,000 Ncc/h $g_{active\ phase}$.

catalyst. Fig. 13 summarizes the steady-state $DeNO_x$ performances obtained from the bulk of transient response SCR experiments collected varying the NO_2/NO_x feed ratio between 0 and 1: NO_x conversions at different temperatures (from 185 up to 385 °C) are plotted versus the NO_2/NO_x feed ratio.

It is evident that for each temperature higher than 185 °C, the maximum NO_x conversion was achieved at the NO_2/NO_x feed ratio = 0.5 (i.e. equimolar NO/NO_2 mixture, 500 ppm NO and 500 ppm NO_2) in agreement with the results reported by other authors [4,17,18,25,26,40] for both the zeolite and the vanadium catalyst; in contrast, in the low temperature region the increase in the NO_2 feed content resulted in a monotonic increase of the NO_x conversion.

The maximum gain in NO_x conversion could be always obtained by moving from NO_2/NO_x = 0, that is with only NO in the feed, to NO_2/NO_x ratio = 0.5. In this region NO_2 becomes the limiting reactant of the fast SCR: thus, the main reaction prevailing in these conditions is the standard SCR reaction (1), which was shown to be poorly active over the zeolite system, especially at low temperatures, if compared to the fast SCR reaction.

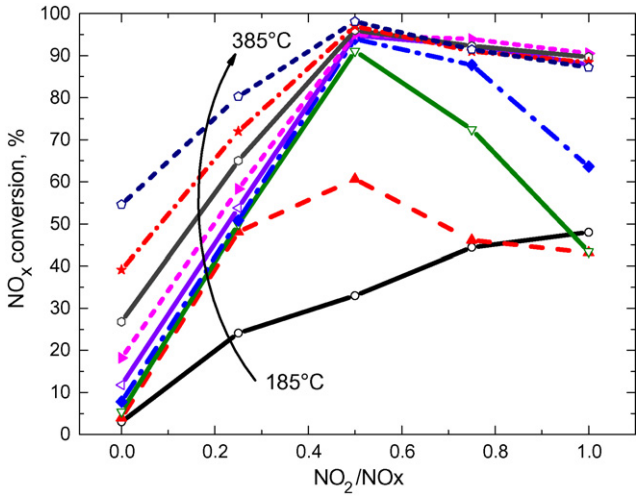

Fig. 13. NO_2/NO_x feed ratio effect on $DeNO_x$ activity over Fe–zeolite crushed monolith. W_{cat} = 0.160 g (0.042 g), Q = 280 Ncc/min, NH_3 = 1000 ppm, NO_x = 1000 ppm, H_2O = 1%, O_2 = 2%. T = 185, 210, 235, 255, 285, 310, 335, 360 and 385 °C.

On the other hand, at $T \geq 250$ °C very high NO_x conversion values were preserved even for NO_2/NO_x ratios > 0.5, due to the high activity of the zeolite catalyst in the NO_2 SCR reaction (7). At low temperatures, the ammonium nitrate formation reaction (6) was also active.

A strong effect of the NO_2/NO_x feed ratio was evident on the N_2O production, and thus on the selectivity of the SCR process. Fig. 14 shows the N_2O concentrations measured in the different experiments as a function of temperature. In agreement with the fact that N_2O comes from the thermal decomposition of ammonium nitrate (reaction (8)), the highest N_2O selectivities were detected in correspondence of large NO_2 to NO_x feed contents.

Finally, to analyze the effects of oxygen (2–10%, v/v) and water (1–10%, v/v) feed contents on the fast SCR reaction additional experiments were run over the monolith core

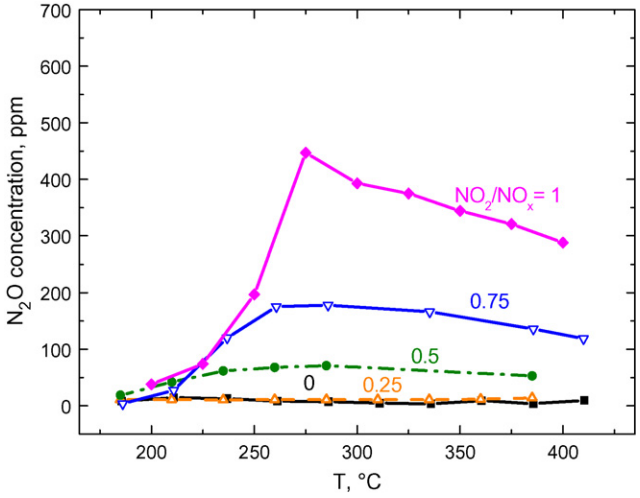

Fig. 14. NO_2/NO_x feed ratio effect on N_2O formation over Fe–zeolite crushed monolith. W_{cat} = 0.160 g (0.042 g), Q = 280 Ncc/min, NH_3 = 1000 ppm, NO_x = 1000 ppm, H_2O = 1%, O_2 = 2%.

Table 1
Effects of the feed composition on the SCR reactivity over the Fe-zeolite catalyst.

Operating variable	Effects
Oxygen concentration (2–10%, v/v)	No effect on NH3 adsorption
	Promotes NH3 oxidation
	Promotes NO oxidation
	Inhibits NO2 adsorption
	Inhibits NO2 decomposition
	Promotes standard SCR
	No effect on fast SCR
Water concentration (1–10%, v/v)	No effect on NH3 adsorption
	Inhibits NH3 oxidation
	Inhibits NO oxidation
	Promotes NO_2 adsorption
	Inhibits NO_2 decomposition
	No effect on standard SCR
	Promotes fast SCR
NH_3 concentration	Low NH_3 concentration promotes standard SCR
	Low NH_3 concentration promotes fast SCR
NO_2/NO_x feed ratio	$T < 220$ °C: behaviour dominated by reactivity of NO_2
	High T: maximum DeNOx @ $NO_2/NO_x = 0.5$

samples feeding 1000 ppm of NH_3 and 1000 ppm of $NO_x = NO + NO_2$, with a 1/1 NO/NO_2 feed ratio. The data (not reported) showed no significant effects of oxygen, while a promoting action of water was apparent in the whole investigated T-range.

The effect of the NH_3 concentration on the fast SCR reaction was addressed, too. The fast SCR activity was enhanced when the ammonia feed concentration was decreased from 1000 to 500 ppm while keeping the NH_3/NO_x feed ratio to one. However such an effect was not dramatic, the observed variation being close to 10% of the total NO_x conversion.

4. Conclusions

A systematic study of the $NH_3/NO–NO_2$ SCR reactivity over a commercial washcoated Fe–zeolite-based catalyst, in view of its use in diesel exhausts aftertreatment technologies, was presented in this paper. Transient experiments involving reacting systems of growing complexity ($NH_3 + O_2$, $NO + O_2$, $NO_2 + O_2$, $NH_3 + NO + O_2$, $NH_3 + NO_2 + O_2$ and $NH_3 + NO + NO_2 + O_2$) were performed in the representative 150–550 °C temperature range over catalyst samples both in powder form (obtained by crushing the original monolith), to derive intrinsic kinetic information, and in form of small core monoliths under isothermal steady-state conditions: the effects of the main operating conditions (temperature, oxygen and water feed contents, NH_3/NO_x feed ratio and NO_2/NO_x feed ratio) were tested, and the main results are qualitatively summarized in Table 1.

The results were also compared to those collected during previous work on a commercial extruded V-based SCR catalyst. The zeolite system was characterized by: (i) higher NH_3 storage capacity, and ability to retain ammonia adsorbed species up to higher temperatures; (ii) higher activity in NH_3 oxidation, with stronger O_2 dependence; (iii) activity in the NO oxidation to NO_2, which was not observed over the V-based system; (iv) higher activity in the standard SCR reaction at low temperature; (v) stronger NO_2 promoting effect and higher activity in the fast SCR reaction; (vi) higher selectivity to N_2O in the presence of excess NO_2.

Acknowledgements

The authors wish to thank DaimlerChrysler for financial support and for permission to publish this work. Useful discussions with Daniel Chatterjee, Michel Weibel, Brigitte Bandl-Konrad and Bernd Krutzsch are also gratefully acknowledged.

References

[1] ACEA final report on Selective Catalytic Reduction – June 2003 – http://europa.eu.int/comm/enterprise/automotive/mveg_meetings/meeting94/scr_paper_final.pdf.
[2] http://www.cleers.org.
[3] http://www.sae.org/automag/features/futurelook/01-2005/1-113-1-84.pdf.
[4] M. Koebel, G. Madia, M. Elsener, Catal. Today 73 (2002) 239.
[5] I. Nova, C. Ciardelli, E. Tronconi, D. Chatterjee, B. Bandl-Konrad, Catal. Today 114 (2006) 3.
[6] P. Forzatti, L. Lietti, E. Tronconi, in: I.T. Horvath (Ed.), Nitrogen Oxides Removal—Industrial. Encyclopaedia of Catalysis, first ed., Wiley, New York, 2002, , and references therein.
[7] G. Madia, M. Koebel, M. Elsener, A. Wokaun, IEC Res. 41 (2002) 3512–3517.
[8] D. Chatterjee, T. Burkhardt, B. Bandl-Konrad, T. Braun, E. Tronconi, I. Nova, C. Ciardelli, SAE Technical Paper 2005-01-965 (2005).
[9] D. Chatterjee, T. Burkhardt, M. Weibel, E. Tronconi, I. Nova, C. Ciardelli, SAE Technical Paper 2006-01-0468 (2006).
[10] C. Ciardelli, I. Nova, E. Tronconi, D. Chatterjee, T. Burkhardt, M. Weibel, Chem. Eng. Sci. 62 (2007) 5001–5006.
[11] L. Chimielarz, P. Kuśtrowski, R. Dziembaj, P. Cool, E.F. Vasant, Appl. Catal. B: Environ. 62 (2006) 369.
[12] R. Moreno-Tost, J. Santamaria-González, E. Rodriguez-Castellón, A. Jiménez-López, M.A. Autié, E. González, M. Carreras Glacial, C. De las Pozas, Appl. Catal. B: Environ. 50 (2004) 279.
[13] J.G. Qi, J.E. Gatt, R.T. Yang, J. Catal. 226 (2004) 120.
[14] R.Q. Long, R.T. Yang, J. Catal. 201 (2001) 145.
[15] O. Kröcher, M. Devadas, M. Elsener, A. Wokaun, N. Söger, M. Pfeifer, Y. Demel, L. Mussmann, Appl. Catal. B: Environ. 66 (2006) 208.
[16] H. Sjövall, L. Olsson, E. Fridell, R.J. Blint, Appl. Catal. B: Environ. 64 (2006) 180.
[17] Y.H. Yeom, J. Henao, Me.J. Li, W.M.H. Sachtler, E. Weitz, J. Catal. 231 (2005) 181.
[18] M. Devadas, O. Kröcher, M. Elsener, A. Wokaun, N. Soger, M. Pfeifer, Y. Demel, L. Mussmann, Appl. Catal. B: Environ. 67 (2006) 187.
[19] G. Delahay, D. Valade, A. Guzmán-Vargas, B. Coq, Appl. Catal. B: Environ. 55 (2005) 149.
[20] R.Q. Long, R.T. Yang, J. Catal. 207 (2002) 224.
[21] M.S. Kumar, M. Schwidder, W. Grünert, U. Bentrup, A. Brückner, J. Catal. 239 (2006) 173.
[22] M. Schwidder, M.S. Kumar, K. Klementiev, M.M. Pohl, A. Brückner, W. Grünert, J. Catal. 231 (2005) 314.

[23] J.A. Sullivan, J. Cunningham, M.A. Morris, K. Keneavey, Appl. Catal. B: Environ. 7 (1995) 137.
[24] M. Wallin, C.J. Karlsson, M. Skoglundh, A. Palmqvist, J. Catal. 218 (2003) 354.
[25] G. Piazzesi, O. Krocher, M. Elsener, A. Wokaun, Appl. Catal. B: Environ. 65 (2006) 55.
[26] G. Piazzesi, O. Krocher, M. Elsener, A. Wokaun, Appl. Catal. B: Environ. 65 (2006) 169.
[27] C. Ciardelli, I. Nova, E. Tronconi, B. Konrad, D. Chatterjee, K. Ecke, M. Weibel, Chem. Eng. Sci. 59 (2004) 5301.
[28] E. Tronconi, I. Nova, C. Ciardelli, D. Chatterjee, B. Bandl-Konrad, T. Burkhardt, Catal. Today 105 (2005) 529.
[29] I. Nova, C. Ciardelli, E. Tronconi, D. Chatterjee, B. Bandl-Konrad, AIChE J. 52 (2006) 3222.
[30] C. Ciardelli, I. Nova, E. Tronconi, B. Bandl-Konrad, D. Chatterjee, M. Weibel, B. Krutzsch, Appl. Catal B: Environ. 70 (1–4) (2007) 80.
[31] E. Tronconi, I. Nova, C. Ciardelli, D. Chatterjee, M. Weibel, J. Catal. 245 (2007) 1.
[32] D. Chatterjee, T. Burkhardt, M. Weibel, I. Nova, A. Grossale, E. Tronconi, SAE Technical Paper, 2007-01-1136 (2007).
[33] I. Nova, C. Ciardelli, E. Tronconi, D. Chatterjee, M. Weibel, Top. Catal. 42–43 (1–4) (2007) 43.
[34] C. Ciardelli, I. Nova, E. Tronconi, M. Ascherfeld, W. Fabinski, Top. Catal. 42–43 (1–4) (2007) 161.
[35] S. Djerad, M. Crocoll, S. Kureti, L. Tifouti, W. Weisweiler, Catal. Today 113 (2006) 208.
[36] N. Apostolescu, T. Schroder, S. Kureti, Appl. Catal. B: Environ. 51 (2004) 43.
[37] J. Despres, M. Koebel, O. Krocker, M. Elsener, A. Wokaun, Appl. Catal. B: Environ. 43 (2003) 389.
[38] I. Nova, L. Castoldi, L. Lietti, E. Tronconi, P. Forzatti, F. Prinetto, G. Ghiotti, J. Catal. 222 (2004) 377.
[39] P. Pascal, Nouveau traité de Chimie Minérale, Masson et C. Editeurs, Tome X (1956) 208.
[40] M. Koebel, M. Elsener, G. Madia, Ind. Eng. Chem. Res. 40 (2001) 52.
[41] M. Li, J. Henao, Y. Yeom, E. Weitz, W.M.H. Sachtler, Catal. Lett. 98 (2004) 5.
[42] K. Rahkamaa-Tolonen, T. Maunula, M. Lomma, M. Huuhtanen, R.L. Keiski, Catal. Today 100 (2005) 217.